Study of the hidden-heavy pentaquarks and P_{cs} states

Wen-Xuan Zhang,[1,†] Chang-Le Liu,[1,‡] and Duojie Jia[1,2,3,*]

[1]*Institute of Theoretical Physics, College of Physics and Electronic Engineering, Northwest Normal University, Lanzhou 730070, China*

[2]*General Education Center, Qinghai Institute of Technology, Xining 810000, China*

[3]*Lanzhou Center for Theoretical Physics, Lanzhou University, Lanzhou 730000, China*

(Received 22 December 2023; accepted 16 May 2024; published 24 June 2024)

Inspired by the recently observed resonance states $P^{\Lambda}_{\psi s}(4338)^0$ and $P_{cs}(4459)^0$ by LHCb Collaboration in $J/\psi\Lambda$ decay channel, we perform a systematical study of all possible hidden-heavy pentaquarks with strangeness $S = 0, -1, -2, -3$, in unified framework of MIT bag model. The color-spin wave functions in terms of Young-Yamanouchi bases and transformed into baryon-meson couplings are utilized to calculate masses, magnetic moments, and relative partial widths of the hidden-heavy pentaquarks, suggesting that the observed $P^{\Lambda}_{\psi s}(4338)^0$ is likely to be a $1/2^-$ compact P_{cs} pentaquark, and the $P_{cs}(4459)^0$ favors two-peak structure of $3/2^-$ and $1/2^-$ P_{cs} states. Our computation indicates that hidden-heavy pentaquarks have the masses around 4.35–4.90 GeV for the P_{cs}, 11.21–11.67 GeV for the P_{bs}, 4.73–5.02 GeV for the P_{css}, and 11.54–11.77 GeV for the P_{bss}.

DOI: 10.1103/PhysRevD.109.114037

I. INTRODUCTION

In addition to the conventional hadronic states, such as mesons $q\bar{q}$ and baryons qqq in quark configurations, the possible exotic tetraquarks $q^2\bar{q}^2$ and pentaquarks $q^4\bar{q}$ are also suggested at the birth of quark model [1,2]. Later in the 1970s, the MIT bag model has been developed by Jaffe [3–5] for the study of exotic multiquark states and notation of color confinement. In the past few decades, it has been applied to describe the doubly heavy baryons [6–9] and exotic states, including light pentaquarks [10] and hybrid mesons [11,12]. Despite that these states are considered to be exotic beyond the conventional scheme of quark model, the existences of them are allowed by quantum chromodynamics (QCD).

Since the observation of exotic $X(3872)$ in 2003 by the Belle Collaboration [13], there are many candidates that have been discovered for tetraquarks, such as the $Z_c(3900)$ [14,15] and the $T_{cc}(3875)$ [16], as well as the fully charm systems $X(6600)$ [17] and $X(6900)$ [18]. In 2015, the first evidence for pentaquarklike structures $P_c(4450)^+$ and $P_c(4380)^+$ with a minimal quark constituent of $uudc\bar{c}$ was reported by LHCb in $J/\psi p$ channel [19], for which the former exhibits a two-peak structure resolved into $P_c(4440)^+$ and $P_c(4457)^+$ in 2019. Recently, the LHCb Collaboration has reported two new hidden charm pentaquarks with a single strange flavor, $P^{\Lambda}_{\psi s}(4338)^0$ [20] and $P_{cs}(4459)^0$ [21], both in $J/\psi\Lambda$ channel. These pentaquark candidates encourage the theoretical study on their mass spectrum, hadron properties, and decay behaviors. There are various pictures and methods applied to analyze the hidden-charm pentaquarks, including molecular [22–34] and compact scenario [35–39], as well as the hidden-bottom pentaquarks [40,41].

For strange hidden-charm pentaquarks with $IJ^P = 0\frac{1}{2}^-$, Ref. [35] predicts some higher states (one with 4386 MeV) that are closer in mass to the measured $P^{\Lambda}_{\psi s}(4338)$ state, and three lower states around 4.1–4.2 GeV. In other two literatures [36,37], no clear conclusion is drawn regarding the $P^{\Lambda}_{\psi s}(4338)$ state. In the case of the $P_{cs}(4459)$, Ref. [35] disfavors splitting of it into two states, while Ref. [36] employs two diquark models to predict a set of low-lying P_{cs} states with six of them closer to 4459 MeV in mass. Reference [37] has discussed the state $P_c(4457)$ merely and gives respective mass predictions.

The purpose of this work is to systematically study masses, magnetic moments, and relative partial widths for hidden-heavy pentaquarks, classified by the strangeness $S = 0, -1, -2, -3$, namely $nnnQ\bar{Q}$, $nnsQ\bar{Q}$, $ssnQ\bar{Q}$, and $sssQ\bar{Q}$, respectively. With the unified framework of the MIT bag model, by which one can address compact configurations of multiquark states without introducing

*Corresponding author: jiadj@nwnu.edu.cn
†zhangwx89@outlook.com
‡liuchanglelcl@qq.com

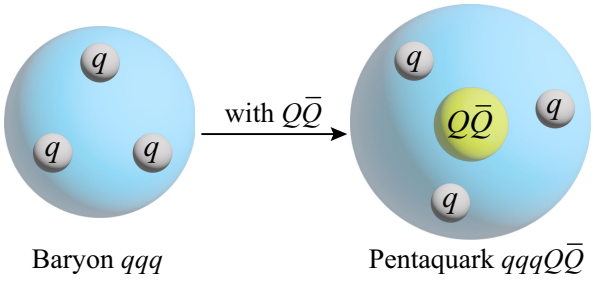

FIG. 1. The relationship of inner-structures between light-flavor baryon and hidden-heavy pentaquark.

new interactions, we compute the masses, magnetic moments for hidden-heavy pentaquarks, with the help of the Young tableau and Young-Yamanouchi bases for the color-spin wave functions. Transforming the color-spin wave functions into that of color-singlet (baryon-meson coupling) and color-octet components, we compute relative partial width of the hidden-heavy pentaquarks. Our mass computation of the P_{cs} states agrees reasonably with the measured values of these states.

In computation of this work, we utilize the variational method to solve the bag model for the hidden-heavy pentaquarks, which includes relativisitc kinematics and interactions inspired by QCD and has relatively less parameters. The model paramaters were fixed in our previous work [42] via matching the observed S-wave masses of all conventional mesons and baryons (including Ξ_{cc}^{++}) and applied to the tetraquarks [43] and full-heavy pentaquarks [44]. As demonstrated in Fig. 1, we extend the bag picture for a light-flavor baryon qqq ($q = u, d, s$) to that of a hidden-heavy pentaquark $qqq\bar{Q}$, with insertion of heavy $Q\bar{Q}$ ($Q = c, b$) in the former. We assume the bag picture of light baryons to hold for the hidden-heavy system of $qqqQ\bar{Q}$ due to suppression of relativistic effects in the dynamics of heavy quark pair.

This work is structured as follows. In Sec. II, we provide a brief introduction to the fundamental relations of the Hamiltonian and magnetic moment. Additionally, we outline the parameters utilized in our numerical calculations. The detailed formulations about the chromomagnetic structure and magnetic moment can be found in the Appendix. In Sec. III, we present a comprehensive numerical analysis of hidden-heavy pentaquarks, with Secs. III A, III B, III C, and III D corresponding to the case of strangeness $S = 0, -1, -2, -3$, respectively. Finally, this work ends with a summary in Sec. IV.

II. FORMULATION FOR MASS, MAGNETIC MOMENT AND DECAY

In the framework of the MIT bag model, all valence quarks are confined within a spherical bag characterized by a radius R and respective momentum x_i. These quarks are coupled each other by perturbative chromomagnetic interactions due to exchange of the lowest-order gluons, as described in the Refs. [5,45]. The mass formula associated with the bag, representing a hadronic state, is given by

$$M(R) = \sum_i \omega_i + \frac{4}{3}\pi R^3 B - \frac{Z_0}{R} + M_{\rm BD} + M_{\rm CMI}, \quad (1)$$

$$\omega_i = \left(m_i^2 + \frac{x_i^2}{R^2}\right)^{1/2}. \quad (2)$$

Here, in Eq. (1), the first term represents the sum of the kinetic energy for the relativistic quark i with mass m_i, the second is volume energy with bag constant B, which characterizes the difference between perturbative and nonperturbative QCD vacuum, the third is zero point energy with coefficient Z_0, the forth accounts for the binding energy between heavy quarks or heavy and strange quarks [46–49], and the fifth represents the chromomagnetic interaction [50]. The bag radius R is the only variable to be determined by minimizing Eq. (1). The momentum x_i, given in units of R^{-1}, satisfies a boundary condition on the bag surface

$$\tan x_i = \frac{x_i}{1 - m_i R - (m_i^2 R^2 + x_i^2)^{1/2}}, \quad (3)$$

which can be derived by quark spinor wave function.

The interactions among quarks involved in this work have two primary components: the lowest-order gluon exchange and short-range effects [50]. For the first part, the binding energies $M_{\rm BD}$ primarily arise from short-range chromoelectric interactions between heavy quarks or heavy-strange systems, both of which are massive and moving nonrelativistically. Specifically, we incorporate four binding energies B_{cs}, B_{cc}, B_{bs}, and B_{bb} in color $\bar{\mathbf{3}}_c$ representation for hidden-heavy pentaquarks, and scale them to other color configurations by the color factors [46,48]. The second component involves chromomagnetic interaction $M_{\rm CMI}$, which contributes to the overall dynamics of the system. The interaction arising from the magnetic moments of quark spin can be described by the following typical form:

$$M_{\rm CMI} = -\sum_{i<j} \langle \boldsymbol{\lambda_i} \cdot \boldsymbol{\lambda_j} \rangle \langle \boldsymbol{\sigma_i} \cdot \boldsymbol{\sigma_j} \rangle C_{ij}, \quad (4)$$

where i and j represent the indices of the quarks (or antiquarks), λ denotes the Gell-Mann matrices, σ signifies the Pauli matrices, and C_{ij} corresponds to the chromomagnetic interaction (CMI) parameters as defined in Ref. [42]. The color and spin factors (the averaged values of Casimir operator) in Eq. (4) are calculable utilizing the method in Refs. [42–44], with the color-spin wave functions given in Appendix A.

Next, we briefly review the formulations of magnetic moment of a multiquark. In the context of the MIT bag model, the magnetic moment of an individual quark depends upon the parameters (R, m_i, x_i) that satisfy some boundary conditions [5]. The radial wave function solution to Eq. (1) for the quark i is given by the spinor wave function,

$$\psi_i(r) = N_i \begin{pmatrix} j_0(x_i r/R)U \\ i\frac{x_i}{(\omega_i+m_i)R} j_1(x_i r/R)\boldsymbol{\sigma}\cdot\hat{\mathbf{r}}U \end{pmatrix} e^{-i\omega_i t}. \quad (5)$$

Applying the operator $\boldsymbol{r}\times\boldsymbol{\gamma}$ to the wave function (5) gives the magnetic moment for the ith quark:

$$\begin{aligned}\mu_i &= \frac{Q_i}{2}\int_{\text{bag}} \mathrm{d}^3 r\bar{\psi}_i(\boldsymbol{r}\times\boldsymbol{\gamma})\psi_i \\ &= \frac{Q_i}{2}\int_0^R \mathrm{d}r r^2 \int \mathrm{d}\Omega\bar{\psi}_i(\boldsymbol{r}\times\boldsymbol{\gamma})\psi_i \\ &= Q_i\frac{R}{6}\frac{4\omega_i R + 2m_i R - 3}{2\omega_i R(\omega_i R-1)+m_i R}, \end{aligned} \quad (6)$$

where Q_i is electric charge of the quark, and $\boldsymbol{\gamma}$ are the Dirac matrices. Then, it is straightforward to apply Eq. (6) to calculate the magnetic moment for each flavor of quark with mass m_i and parameters (R, x_i) determined.

For a hadron with wave function $|\psi\rangle$, which are formed by the color-spin wave functions given in Table IX and the radial wave functions in Eq. (5), its magnetic moment is defined as [51]

$$\mu = \langle\psi|\hat{\mu}|\psi\rangle, \qquad \hat{\mu} = \sum_i g_i\mu_i\hat{S}_{iz}, \quad (7)$$

with $g_i = 2$, and $\hat{S}_{iz}$ denotes the third component of spin for an individual quark. Application of Eqs. (7) and (6) gives rise to a weighted sum of Eq. (6) in terms of the spin wave functions χ_a $(a = 1, 2, \ldots, 10)$ given explicitly by Eq. (A5) in Appendix A. When color-spin configurations mix chromomagnetically, the sum in Eq. (7) becomes a double sum of a nondiagonal matrices μ_{ab} of magnetic moment in spin space, which are listed explicitly in Table X $(a, b = 1,2, \ldots, 5)$ and XI $(a, b = 6,7, \ldots, 10)$. For more details, see Apppendix B. We use Eq. (7) and Table IX, together with Table X and XI, to compute numerically magnetic moments of the hidden-heavy pentaquarks. The results are listed in Table I through Table VIII, given in unit of the magnetic moment μ_N $(= \mu_p/2.79285$ [52,53]) of nucleon.

In numerical calculations, we proceed with model parameters from a previous work [42] that successfully reconcile the ground-state masses of light hadrons and heavy hadrons and applied to the fully heavy tetraquarks and pentaquarks [43,44]. The chosen constants and masses for quarks with flavor n (light nonstrange flavor $n = u, d$), strange s, charm c, and bottom b are as follows:

$$\left\{\begin{array}{ll} Z_0 = 1.83, & B^{1/4} = 0.145 \text{ GeV}, \\ m_n = 0 \text{ GeV}, & m_s = 0.279 \text{ GeV}, \\ m_c = 1.641 \text{ GeV}, & m_b = 5.093 \text{ GeV}. \end{array}\right\} \quad (8)$$

Meanwhile, we use the binding energies between quarks in the color $\overline{\mathbf{3}}_c$ representation,

$$\left\{\begin{array}{ll} B_{cs} = -0.025 \text{ GeV}, & B_{cc} = -0.077 \text{ GeV}, \\ B_{bs} = -0.032 \text{ GeV}, & B_{bb} = -0.128 \text{ GeV}, \end{array}\right\} \quad (9)$$

and the binding energies between quarks in other color representations via scaling the above values by relative color factors between two reps. Given the parameters in Eqs. (8) and (9), one can perform variational analysis upon Eq. (1) numerically to determine the bag radius R and solve Eq. (3) to find respective momentum x_i for pentaquarks with quantum numbers IJ^P. Having solved parameters (R, x_i), one can then compute the masses and magnetic moments for the given flavor and quantum number J^P of the considered hidden-heavy pentaquarks, as detailed in Sec. III.

Before discussing on hadron properties, it is of importance to exclude scattering states, which is trivial in the common sense of the bound state. The emergence of the scattering states stems from the leak-free choice of bases for the wave function of the considered multiquark. Indeed, the chromomagnetic interaction allows pentaquarks $nnnQ\bar{Q}$ to exhibit some eigenstates ranging from three to five, whereas some of them are very broad and thereby are loosely bound and inherently unstable against dissociation to two separated hadrons. To filter these states, one can examine the color-spin wave function $|\psi\rangle$ in the space of the corresponding bases and eigenvectors empoyed in this work. One can expand a pentaquark state $|\psi\rangle$ in terms of color-singlet $\mathbf{1}_c$ rep. and the color-octet $\mathbf{8}_c$ rep. as follows:

$$|\psi\rangle = c^1|q_1q_2q_3\rangle^{\mathbf{1}}_{S_1}|q_4\bar{q}_5\rangle^{\mathbf{1}}_{S_2} + c^8|q_1q_2q_3\rangle^{\mathbf{8}}_{S_3}|q_4\bar{q}_5\rangle^{\mathbf{8}}_{S_4} + \ldots, \quad (10)$$

in which the first component stands for the fock state of a colorless baryon and a colorless meson (with spin S_1 and S_2), with the coefficient c^1 the overlap of the wave function obtained via diagonalization of chromomagnetic interaction matrix, and … stands for sum of the components with other spin configurations. When the probability $|c^1|^2$ approaches 1, the above equation indicates that the pentaquark couples strongly to a scattering state and is quite easy to dissociate into a meson and a baryon. One can regard the first component in Eq. (10) as a scattering state and denote

TABLE I. Calculated spectra (in GeV) of pentaquarks $nnnb\bar{b}$. Bag radius R_0 is in GeV^{-1}. Magnetic moments are in units of μ_N and organized in the order of $I_3 = 3/2, 1/2, -1/2, -3/2$ for $I = 3/2$, or $I_3 = 1/2, -1/2$ for $I = 1/2$. The numbers below respective decay channels are ratios of partial width. The states denoted by asterisks couple strongly to scattering states.

		$nnnb\bar{b}$			$nnn \otimes b\bar{b}$				$nnb \otimes n\bar{b}$					
I	J^P	R_0	M	μ	$\Delta\Upsilon$	$\Delta\eta_b$	$N\Upsilon$	$N\eta_b$	$\Sigma_b^* B^*$	$\Sigma_b^* B$	$\Sigma_b B^*$	$\Sigma_b B$	$\Lambda_b B^*$	$\Lambda_b B$
3/2	$5/2^-$	5.52	11.235		*									
	$3/2^-$	5.53	11.561	1.99, 0.99, 0.00, −0.99	0	1			1	0.58	0.18			
		5.52	11.235		*									
		5.50	11.230			*								
	$1/2^-$	5.57	11.583	0.64, 0.27, −0.10, −0.47	1				1		0.15	0.03		
		5.50	11.539	0.68, 0.39, 0.10, −0.19	1				1		13.43	5.92		
		5.52	11.233		*									
1/2	$5/2^-$	5.52	11.431	2.96, 0.00					1					
	$3/2^-$	5.50	11.412	2.78, −0.04			1		2.48	1	0.66		1	
		5.46	11.394	2.18, 0.05			1		0.07	1	3.25		1	
		5.45	11.333	1.09, −0.01			1		0.27	1	0.09		1	
		5.43	10.929				*							
	$1/2^-$	5.46	11.380	1.49, 0.01			1	3.64	1		1.23	1.31	1	0.08
		5.43	11.323	0.80, −0.06			1	0.0005	1		0.22	1.23	1	1.81
		5.42	11.314	−0.03, 0.06			1	14.66	1		4.78	5.36	1	0.77
		5.42	10.929				*							
		5.41	10.923					*						

TABLE II. Calculated spectra (in GeV) of pentaquarks $nnnc\bar{c}$. Bag radius R_0 is in GeV^{-1}. Magnetic moments are in units of μ_N and organized in the order of $I_3 = 3/2, 1/2, -1/2, -3/2$ for $I = 3/2$, or $I_3 = 1/2, -1/2$ for $I = 1/2$. The numbers below respective decay channels are ratios of partial width. The states denoted by asterisks couple strongly to scattering states.

		$nnnc\bar{c}$			$nnn \otimes c\bar{c}$				$nnc \otimes n\bar{c}$					
I	J^P	R_0	M	μ	$\Delta J/\psi$	$\Delta\eta_c$	NJ/ψ	$N\eta_c$	$\Sigma_c^* D^*$	$\Sigma_c^* D$	$\Sigma_c D^*$	$\Sigma_c D$	$\Lambda_c D^*$	$\Lambda_c D$
3/2	$5/2^-$	5.81	4.547		*									
	$3/2^-$	5.82	4.758	2.23, 1.12, 0.00, −1.12	0	1			1	0.53	0.13			
		5.81	4.547		*									
		5.71	4.503			*								
	$1/2^-$	5.91	4.820	1.59, 1.07, 0.56, 0.04	1				1		0.09	0.02		
		5.76	4.703	−0.01, −0.27, −0.52, −0.78	1				1		36.85	10.1		
		5.75	4.524		*									
1/2	$5/2^-$	5.85	4.661	3.13, 0.00					1					
	$3/2^-$	5.83	4.630	2.85, 0.29			1		4.13	1	0.26		1	
		5.74	4.569	1.69, −0.55			1		0.02	1	19.36		1	
		5.68	4.503	1.83, 0.27			1		⋯	1	0.56		1	
		5.73	4.241				*							
	$1/2^-$	5.80	4.580	1.18, −0.08			1	0.39	1.32		1	0.25	1	0.14
		5.70	4.490	0.06, 0.25			1	10.99	⋯		1	0.01	1	9.3
		5.61	4.452	1.12, −0.18			1	2.73	⋯		⋯	1	1	0.004
		5.71	4.235				*							
		5.59	4.191					*						

it with an asterisk, as shown in Tables I and II for the corresponding decay channels.

Apart from stability research, the eigenvectors c_i play a crucial role in investigating decay to the respective decay channel. Drawing from previous studies [35,54–56], we employ a width formula for the (L-wave) two-body decay [57]:

$$\Gamma_i = \gamma_i \alpha \frac{k^{2L+1}}{m^{2L}} \cdot |c_i|^2, \tag{11}$$

where Γ_i represents the partial width of the channel i, γ_i is prefactor associated with decay dynamics, α describes the coupling strength of the two-body decay, m stands for the mass of initial state, k for the momentum of final states in

the rest frame, and c_i denotes the coefficient of the respective channel when the initial state expanded in terms of the final states of decay channel is considered. For S-wave OZI-superallowed decay mode [3,10], for which we will address in this work, Eq. (11) becomes $\Gamma_i = \gamma_i \alpha k \cdot |c_i|^2$, where k satisfies the following energy relation

$$m_A = \sqrt{m_B^2 + k^2} + \sqrt{m_C^2 + k^2}, \tag{12}$$

for the decaying process $A \to B + C$, and c_i is to be extracted from the coefficient c^1 in Eq. (10) corresponding to the given spin configuration. The coefficient γ_i that depends on spatial wave functions of initial and final states remains unchanged approximately between vector and scalar mesons.

Additionally, in the heavy quark limit, γ_i also remains the same between Σ_c^* and Σ_c [55]. This implies then the following relations:

$$\begin{aligned}
&\gamma_{\Delta\Upsilon} = \gamma_{\Delta\eta_b}, \qquad \gamma_{N\Upsilon} = \gamma_{N\eta_b},\\
&\gamma_{\Delta J/\psi} = \gamma_{\Delta\eta_c}, \qquad \gamma_{NJ/\psi} = \gamma_{N\eta_c},\\
&\gamma_{\Sigma_b^* B^*} = \gamma_{\Sigma_b^* B} = \gamma_{\Sigma_b B^*} = \gamma_{\Sigma_b B},\\
&\gamma_{\Sigma_c^* D^*} = \gamma_{\Sigma_c^* D} = \gamma_{\Sigma_c D^*} = \gamma_{\Sigma_c D},\\
&\gamma_{\Lambda_b B^*} = \gamma_{\Lambda_b B}, \qquad \gamma_{\Lambda_c D^*} = \gamma_{\Lambda_c D}.
\end{aligned} \tag{13}$$

These approximate relations enable us to explore the relative partial widths via estimating the factors $k \cdot |c_i|^2$. The computed results are listed in Table I through Table VIII, corresponding to respective decay channels shown there. We denote all forbidden processes due to mass conservation by a short dash in these tables.

III. MASSES AND OTHER PROPERTIES: NUMERICAL RESULTS

A. The $nnnQ\bar{Q}$ systems

We first consider the nonstrange $nnnQ\bar{Q}$ $(Q = c,b)$ pentaquarks, with n denoting the up and down quarks. It is straightforward to find the masses and magnetic moments of this system with the variational method applied to the MIT bag model, which includes the chromomagnetic interactions, and using Eq. (7). For partial width and stability, we apply the bases of pentaquark in Ref. [35] to explore the components composed of colorless baryons and colorless mesons in expansion of the wave functions. The numerical results are tabulated in Tables I and II.

Upon the completion of numerical computations, we proceed to discuss the mass spectra and label a $nnnQ\bar{Q}$ pentaquark state into symbol $P_Q(I, J^P, M)$. The scattering states exhibiting the lowest mass splittings, such as $P_b(1/2, 1/2^-, 10.923)$ and $P_c(1/2, 1/2^-, 4.191)$, restrict the mass range to 11.31–11.58 GeV for the $nnnb\bar{b}$ and to 4.45–4.82 GeV for the $nnnc\bar{c}$. Obviously, the predicted mass gap of 270 MeV in the b sector is narrower than that of 370 MeV in the c sector, being in consistent with the suppression of heavy quark. However, the measured masses do not fall within the range of our computed mass, as indicated by the following observed data [58,59,19] for states which may carry negative parity:

$$\begin{aligned}
&P_c(4312)^+ M = 4312\ \text{MeV}\,\Gamma = 9.8\ \text{MeV},\\
&P_c(4337)^+ M = 4337\ \text{MeV}\,\Gamma = 29\ \text{MeV},\\
&P_c(4380)^+ M = 4380\ \text{MeV}\,\Gamma = 215\ \text{MeV},
\end{aligned} \tag{14}$$

all below the state $P_c(1/2, 1/2^-, 4.452)$ in mass. This suggests that they are unlikely to be compact pentaquarks, which we assume in the bag model. This is in consistent with the molecular picture suggested by a set of Refs. [60–64].

Nevertheless, there are several states that appear to be compact potentially. These states include the low-lying states of the $P_b(1/2, 1/2^-, 11.380)$, the $P_b(1/2, 1/2^-, 11.323)$ and $P_b(1/2, 1/2^-, 11.314)$ in the hidden-bottom systems and the states $P_c(1/2, 1/2^-, 4.580)$, the $P_c(1/2, 1/2^-, 4.490)$ and the $P_c(1/2, 1/2^-, 4.452)$ in the hidden-charm systems. Considering the components of $nnn \otimes c\bar{c}$ of the hidden-charm pentaquaks, which have three masses, one can determine the ratios of partial widths between the decaying channels $N\eta_c$ and NJ/ψ. Results are

$$\begin{aligned}
&\frac{\Gamma(P_c(1/2, 1/2^-, 4.580) \to N\eta_c)}{\Gamma(P_c(1/2, 1/2^-, 4.580) \to NJ/\psi)} = 0.39,\\
&\frac{\Gamma(P_c(1/2, 1/2^-, 4.490) \to N\eta_c)}{\Gamma(P_c(1/2, 1/2^-, 4.490) \to NJ/\psi)} = 10.99,\\
&\frac{\Gamma(P_c(1/2, 1/2^-, 4.452) \to N\eta_c)}{\Gamma(P_c(1/2, 1/2^-, 4.452) \to NJ/\psi)} = 2.73,
\end{aligned} \tag{15}$$

which favor potentially the decay into $N\eta_c$ channel for the $P_c(1/2, 1/2^-, 4.490)$ and the $P_c(1/2, 1/2^-, 4.452)$. Notably, some states exhibit dominant channels, such as $P_b(1/2, 1/2^-, 11.323)$ decaying into $N\Upsilon$ or the P_b states with $(I)J^P = (3/2)3/2^-$ decaying into $\Delta\eta_b$. If experiments report resonances with masses close to our predictions but in the opposite decay channel, this might either exclude them from our predicted spectrum or explain them as compact pentaquarks. In the $nnQ \otimes n\bar{Q}$ coupling, the decay behaviors are studied, awaiting confirmation through experimental findings. Particularly, the state $P_c(1/2, 1/2^-, 4.452)$ with limited decay channels $\Sigma_c D$ and $\Lambda_c D^*$ can be discoverable in corresponding processes.

In the fifth column of Tables I and II, we present the magnetic moments of pentaquarks while excluding scattering states. Similar evaluations have been conducted in Refs. [34,39,51] covering various configurations. However, this work does not delve into transition moments as $M1$

TABLE III. Calculated spectra (in GeV) of pentaquarks $nnsb\bar{b}$. Magnetic moments are in units of μ_N and organized in the order of $I_3 = 1, 0, -1$ for $I = 1$, or $I_3 = 0$ for $I = 0$. The bag radius R_0 is determined to be 5.50 GeV^{-1}. The numbers below respective decay channels are ratios of partial width. The states denoted by asterisks couple strongly to scattering states.

		$nnsb\bar{b}$		$nns \otimes b\bar{b}$						$nnb \otimes s\bar{b}$					
I	J^P	M	μ	$\Sigma^*\Upsilon$	$\Sigma^*\eta_b$	$\Sigma\Upsilon$	$\Sigma\eta_b$	$\Lambda\Upsilon$	$\Lambda\eta_b$	$\Sigma_b^* B_s^*$	$\Sigma_b^* B_s$	$\Sigma_b B_s^*$	$\Sigma_b B_s$	$\Lambda_b B_s^*$	$\Lambda_b B_s$
1	$5/2^-$	11.524	3.19, 0.24, −2.70	1						1					
		11.378		*											
	$3/2^-$	11.654	0.59, −0.14, −0.86	0	1	0.0001				1.43	1	0.25			
		11.510	2.60, 0.10, −2.41	1.38	1	7.28				4.42	1	0.29			
		11.490	1.96, 0.04, −1.88	0.09	1	0.36				0.04	1	8.18			
		11.464	2.51, 0.59, −1.33	2.48	1	7.27				0.1	1	0.04			
		11.378		*											
		11.373			*										
		11.137				*									
	$1/2^-$	11.675	0.12, −0.15, −0.42	1		0.004	0.004			1		0.15	0.03		
		11.635	0.27, 0.06, −0.15	1		0.006	0.004			1		16.45	8.56		
		11.488	1.45, 0.14, −1.18	1		4.57	3.06			1		0.81	0.2		
		11.452	−0.69, −0.39, −0.09	1		47.08	83.87			1		1.45	0.19		
		11.445	2.03, 0.59, −0.85	1		5.93	21.13			0.05		1	28.8		
		11.376		*											
		11.137				*									
		11.131					*								
0	$5/2^-$	11.590	0.24												
	$3/2^-$	11.538	0.24					1						1	
		11.521	0.40					1						1	
		11.447	0.19					1						1	
		11.262	−0.25					1						1	
		11.094						*							
	$1/2^-$	11.505	0.26					1	8.85					1	0.05
		11.439	0.39					1	0.003					1	1.21
		11.429	−0.24					1	27.57					1	1.29
		11.259	−0.09					1	0.71					1	0.002
		11.210	−0.08					1	3.24					0.002	1
		11.094						*							
		11.088							*						

transition processes are typically suppressed against strong decay. The magnetic moments are organized based on the isospin component I_3, ranging from $0.09\mu_N$ to $3.35\mu_N$. This implies that the electric charge of the final states could potentially aid in predicting the specific magnetic moment if the mass and decay channel align with experimental reports.

B. The $nnsQ\bar{Q}$ systems

In the subsequent analysis, we explore the considerable hidden-heavy pentaquarks $nnsQ\bar{Q}$ with a single strange flavor. For these systems, the color-spin bases expand to eight for $I = 1$ and seven for $I = 0$, detailed in Appendix A. Consequently, numerical calculations must rely on the perturbative method of the MIT bag model, where we variate Eq. (1) by treating the M_{CMI} matrix as perturbation. To investigate the decay channels, we employ the relations

$$\begin{aligned}
&\gamma_{\Sigma^*\Upsilon} = \gamma_{\Sigma^*\eta_b} = \gamma_{\Sigma\Upsilon} = \gamma_{\Sigma\eta_b}, \qquad \gamma_{\Lambda\Upsilon} = \gamma_{\Lambda\eta_b},\\
&\gamma_{\Sigma^* J/\psi} = \gamma_{\Sigma^*\eta_c} = \gamma_{\Sigma J/\psi} = \gamma_{\Sigma\eta_c}, \qquad \gamma_{\Lambda J/\psi} = \gamma_{\Lambda\eta_c},\\
&\gamma_{\Sigma_b^* B_s^*} = \gamma_{\Sigma_b^* B_s} = \gamma_{\Sigma_b B_s^*} = \gamma_{\Sigma_b B_s}, \qquad \gamma_{\Lambda_b B_s^*} = \gamma_{\Lambda_b B_s},\\
&\gamma_{\Sigma_c^* D_s^*} = \gamma_{\Sigma_c^* D_s} = \gamma_{\Sigma_c D_s^*} = \gamma_{\Sigma_c D_s}, \qquad \gamma_{\Lambda_c D_s^*} = \gamma_{\Lambda_c D_s}, \quad (16)
\end{aligned}$$

applied to Eq. (11). The results of mass spectrum, magnetic moment and ratios of partial widths are presented in Tables III and IV.

The scattering states entering for each spin parity should be excluded first. Here, we denote a pentaquark state as $P_{Qs}(I, J^P, M)$ in this section. For subsystems with $I = 0$, we identify several scattering states like $P_{bs}(0, 3/2^-, 11.094)$, $P_{bs}(0, 1/2^-, 11.094)$ and $P_{bs}(0, 1/2^-, 11.088)$ for bottom sector, and $P_{cs}(0, 3/2^-, 4.406)$, $P_{cs}(0, 1/2^-, 4.402)$ and $P_{cs}(0, 1/2^-, 4.358)$ for charm sector. In the case of $I = 1$, 13 more scattering states are explicitly marked with asterisks. It is noteworthy that the lightest P_{cs}

TABLE IV. Calculated spectra (in GeV) of pentaquarks $nnsc\bar{c}$. Magnetic moments are in units of μ_N and organized in the order of $I_3 = 1, 0, -1$ for $I = 1$, or $I_3 = 0$ for $I = 0$. The bag radius R_0 is determined to be 5.78 GeV^{-1}. The numbers below respective decay channels are ratios of partial width. The states denoted by asterisks couple strongly to scattering states.

		$nnsc\bar{c}$		$nns \otimes c\bar{c}$						$nnc \otimes s\bar{c}$					
I	J^P	M	μ	$\Sigma^* J/\psi$	$\Sigma^* \eta_c$	$\Sigma J/\psi$	$\Sigma \eta_c$	$\Lambda J/\psi$	$\Lambda \eta_c$	$\Sigma_c^* D_s^*$	$\Sigma_c^* D_s$	$\Sigma_c D_s^*$	$\Sigma_c D_s$	$\Lambda_c D_s^*$	$\Lambda_c D_s$
1	$5/2^-$	4.767	3.36, 0.27, −2.82	1						1					
		4.690		*											
	$3/2^-$	4.863	0.84, −0.08, −0.99	0.0001	1	0.0004				1.18	1	0.15			
		4.751	2.62, 0.42, −1.77	1.16	1	2.03				10.27	1	0.07			
		4.691		*											
		4.683	1.66, −0.46, −2.58	7.26	1	0.3				0	1	28.38			
		4.651	3.70, 0.88, −1.94	0.003	1	0.006				0.0002	1	0.03			
		4.643	2.99, 0.40, −2.19	0.0005	1	0.001				0.02	1	0.73			
		4.451				*									
	$1/2^-$	4.920	0.94, 0.51, 0.08	1		0.002	0.002			1		0.08	0.02		
		4.814	−0.29, −0.52, −0.74	1		0.007	0.002			0.002		1	0.36		
		4.716	1.41, 0.12, −1.16	1		1.43	0.26			1		0.68	0.03		
		4.666		*											
		4.637	−0.39, −0.01, 0.37	1		0.17	10.45			1		6.32	0.69		
		4.594	1.76, 0.16, −1.43	0.0007		1	2.14			⋯		1	15.12		
		4.445				*									
		4.402					*								
0	$5/2^-$	4.792	0.27												
	$3/2^-$	4.757	0.59					1						1	
		4.708	0.19					1						1	
		4.630	0.12					1						1	
		4.494	−0.27					1						1	
		4.406						*							
	$1/2^-$	4.703	0.25					1	0.62					1	0.15
		4.619	0.59					1	3.13					1	21.73
		4.592	−0.42					1	3.57					1	0.02
		4.487	−0.64					1	1.47					1	0.002
		4.402						*							
		4.358							*						
		4.353	0.32					1	2.17					⋯	1

pentaquark $P_{cs}(0, 1/2^-, 4.353)$ remains as a tightly bound state. Accordingly, we have P_{bs} pentaquarks ranging from 11.210 GeV to 11.675 GeV and P_{cs} from 4.353 GeV to 4.920 GeV, each with significant mass splittings of 465 MeV and 567 MeV, respectively, due to the presence of a single strange flavor.

Regarding the P_{cs} pentaquark candidates, LHCb Collaboration has reported two resonances in $J/\psi\Lambda$ final states [20,21]:

$$P^{\Lambda}_{\psi s}(4338)^0 M = 4338.2\ \text{MeV}\,\Gamma = 7.0\ \text{MeV},$$
$$P_{cs}(4459)^0 M = 4458.8\ \text{MeV}\,\Gamma = 17.3\ \text{MeV}, \quad (17)$$

with preferred spin parity $1/2^-$ of the former. By examining the corresponding threshold of $P^{\Lambda}_{\psi s}(4338)^0$, we find that its mass of 4338.2 MeV is slightly higher than $\Xi_c D$, below $\Xi_c' D$ by 108 MeV, and below $\Xi_c D^*$ by 140 MeV. Despite the deep binding of over 100 MeV, suggesting it may not be a molecular state, $P^{\Lambda}_{\psi s}(4338)^0$ can be described as a compact pentaquark $P_{cs}(0, 1/2^-, 4.353)$ with a magnetic moment of $0.32\mu_N$ and ratio of partial widths

$$\frac{\Gamma(P_{cs}(0, 1/2^-, 4.353) \to \Lambda\eta_c)}{\Gamma(P_{cs}(0, 1/2^-, 4.353) \to \Lambda J/\psi)} = 2.17. \quad (18)$$

The spin parity of $P_{cs}(4459)^0$ has not been determined and could be either $3/2^-$ or $1/2^-$, corresponding to predicted $P_{cs}(0, 3/2^-, 4.494)$ and $P_{cs}(0, 1/2^-, 4.487)$, respectively. We are looking forward to further experiments on quantum numbers and decay channel $\Lambda\eta_c$, for confirming the two-peak hypothesis of $P_{cs}(4459)^0$ dissociating into 4454.9 MeV and 4467.8 MeV [21]. Additionally, Fig. 3(b) of Ref. [21] suggests the existence of several P_{cs} states in the 4.6–4.9 GeV region, as predicted in Table IV.

In this work, our focus extends to the examination of P_{bs} pentaquarks, considering their magnetic moments and

decay channels. Due to the lack of evidence and production mechanism, there is no comparison of them to experimental reports. Nonetheless, similar to the presence of a single massive strange flavor in P_{cs} counterparts, the bottom flavor can exhibit deep binding and suppression of relativistic effects compared to strange and charm flavors. Theoretical predictions, especially those related to magnetic moments and decay channels, can serve as guidance for expected findings of compact P_{bs} pentaquarks.

C. The $ssnQ\bar{Q}$ systems

In analogy to the isovector $nnsQ\bar{Q}$ system, a corresponding system can be constructed by reversing the flavors of n and s, resulting in the $ssnQ\bar{Q}$ system with seven and eight color-spin bases for $J^P = 3/2^-$ and $1/2^-$, respectively. The calculations are performed using the perturbative method of the MIT bag model, along with the application of certain relations for partial width study, as expressed below:

$$\begin{aligned}
&\gamma_{\Xi^*\Upsilon} = \gamma_{\Xi^*\eta_b} = \gamma_{\Xi\Upsilon} = \gamma_{\Xi\eta_b}, \qquad \gamma_{\Xi^* J/\psi} = \gamma_{\Xi^*\eta_c} = \gamma_{\Xi J/\psi} = \gamma_{\Xi\eta_c},\\
&\gamma_{\Xi_b^* B_s^*} = \gamma_{\Xi_b^* B_s} = \gamma_{\Xi_b B_s^*} = \gamma_{\Xi_b B_s}, \qquad \gamma_{\Xi_c^* D_s^*} = \gamma_{\Xi_c^* D_s} = \gamma_{\Xi_c D_s^*} = \gamma_{\Xi_c D_s},\\
&\gamma_{\Omega_b^* B^*} = \gamma_{\Omega_b^* B} = \gamma_{\Omega_b B^*} = \gamma_{\Omega_b B}, \qquad \gamma_{\Omega_c^* D^*} = \gamma_{\Omega_c^* D} = \gamma_{\Omega_c D^*} = \gamma_{\Omega_c D}.
\end{aligned} \tag{19}$$

The corresponding results are presented in Tables V and VI.

In this section, we will designate the pentaquark $ssnQ\bar{Q}$ by the symbol $P_{Qss}(J^P, M)$. Beyond the scattering states, our predictions encompass 10 P_{bss} states ranging from 11.545 GeV to 11.747 GeV and 12 P_{css} states spanning 4.727 GeV to 4.968 GeV. These states exhibit mass differences of 202 MeV and 241 MeV, respectively. Through the $ssn \otimes Q\bar{Q}$ coupling, there are several states that can be found dominantly in channel $\Xi^* J/\psi$ ($\Xi^*\Upsilon$), including $P_{css}(1/2^-, 4.808)$, $P_{css}(1/2^-, 4.925)$ and $P_{css}(1/2^-, 5.021)$ for c sector, and $P_{bss}(1/2^-, 11.729)$, $P_{bss}(1/2^-, 11.766)$ for b sector. The lightest P_{css} pentaquark around 4.7 GeV is expected to be firstly reported in experiments either in system $\Xi J/\psi$, $\Xi\eta_c$, $\Xi_c D_s^*$ or $\Omega_c D^*$.

The formation of a molecular state for a P_{Qss} pentaquark proves challenging due to the exchange of mesons $s\bar{s}$, $c\bar{c}$, and $b\bar{b}$, which only offer short-range interactions among constituent hadrons. Additionally, the superthreshold phenomenon further violates this scenario by positive potentials, implying repulsive force between hadrons. Consequently, we infer that the hidden-heavy pentaquarks with strangeness might be discovered as compact states, arisen from the unsatisfied requirements of the molecular scenario.

TABLE V. Calculated spectra (in GeV) of pentaquarks $ssnb\bar{b}$. Magnetic moments are in units of μ_N and organized in the order of $I_3 = 1/2, -1/2$ for $I = 1/2$. The bag radius R_0 is determined to be 5.53 GeV^{-1}. The numbers below respective decay channels are ratios of partial width. The states denoted by asterisks couple strongly to scattering states.

	$ssnb\bar{b}$		$ssn \otimes b\bar{b}$				$nsb \otimes s\bar{b}$				$ssb \otimes n\bar{b}$			
J^P	M	μ	$\Xi^*\Upsilon$	$\Xi^*\eta_b$	$\Xi\Upsilon$	$\Xi\eta_b$	$\Xi_b^* B_s^*$	$\Xi_b^* B_s$	$\Xi_b B_s^*$	$\Xi_b B_s$	$\Omega_b^* B^*$	$\Omega_b^* B$	$\Omega_b B^*$	$\Omega_b B$
$5/2^-$	11.669	0.49, −2.46	1				1				1			
	11.524		*											
$3/2^-$	11.747	−0.26, −0.79	0	1	0.0001		1.54	1	0.3		5.4	2.43	1	
	11.651	0.51, −2.43	7.54	1	43.94		3.6	1	1.79		1.46	0.67	1	
	11.636	0.61, −1.80	0.0007	1	0.003		0.28	1	2.79		0.05	0.52	1	
	11.561	0.32, −0.90	0.21	1	0.19		0.54	1	0.16		2.73	8.89	1	
	11.524		*											
	11.518			*										
	11.283				*									
$1/2^-$	11.766	−0.22, −0.40	1		0.003	0.003	1		0.01	0.12	40.84		5.93	1
	11.729	0.06, −0.13	1		0.005	0.002	1		0.04	0.003	0.21		2.91	1
	11.620	0.41, −1.32	1		1.12	13.65	1		0.34	0.02	0.33		0.51	1
	11.555	0.61, −0.81	1		2.53	0.03	0.04		1	1.71	0.98		0.16	1
	11.545	−0.37, 0.19	1		0.39	4.37	0.39		1	0.67	0.14		0.96	1
	11.521		*											
	11.283				*									
	11.277					*								

TABLE VI. Calculated spectra (in GeV) of pentaquarks $ssnc\bar{c}$. Magnetic moments are in units of μ_N and organized in the order of $I_3 = 1/2, -1/2$ for $I = 1/2$. The bag radius R_0 is determined to be 5.79 GeV^{-1}. The numbers below respective decay channels are ratios of partial width. The states denoted by asterisks couple strongly to scattering states.

	$ssnc\bar{c}$		$ssn \otimes c\bar{c}$				$nsc \otimes s\bar{c}$				$ssc \otimes n\bar{c}$			
J^P	M	μ	$\Xi^* J/\psi$	$\Xi^* \eta_c$	$\Xi J/\psi$	$\Xi \eta_c$	$\Xi_c^* D_s^*$	$\Xi_c^* D_s$	$\Xi_c D_s^*$	$\Xi_c D_s$	$\Omega_c^* D^*$	$\Omega_c^* D$	$\Omega_c D^*$	$\Omega_c D$
$5/2^-$	4.914	0.54, −2.56	1				1				1			
	4.836		*											
$3/2^-$	4.968	−0.11, −0.93	0.0001	1	0.0007		1.49	1	0.19		9.01	2.65	1	
	4.881	0.90, −2.04	2.74	1	3.52		6.67	1	0.47		3.8	1.34	1	
	4.837	0.48, −2.13	30.3	1	0.05		1.18	1	4.53		0.02	0.22	1	
	4.834	0.64, −2.07	35.37	1	0.14		0.07	1	4.12		0.01	0.0005	1	
	4.792			*										
	4.760	−0.28, −0.95	0.05	1	0.62		0.01	1	0.0001		⋯	1	0	
	4.597				*									
$1/2^-$	5.021	0.44, 0.08	1		0.002	0.001	1		0.02	0.12	67.1		4.23	1
	4.925	−0.37, −0.71	1		0.004	0.0004	1		0.06	0.005	0.23		8.31	1
	4.831	0.39, −1.14	1		0.28	0.20	1		2.91	0.48	5.28		2.65	1
	4.808	0.31, −1.33	1		0.002	0.003	1		2.27	3.07	0.01		0.004	1
	4.754	0.68, 0.30	1		7.09	20.99	⋯		1	18.33	⋯		3.27	1
	4.727	−0.68, −1.16	0.0006		1	2.95	⋯		1	0.004	⋯		0.008	1
	4.592				*									
	4.548					*								

D. The $sssQ\bar{Q}$ systems

Finally, when three strange quarks are present, the light degrees of freedom in $sssQ\bar{Q}$ system are all identical in flavor. The strong symmetry of the wave function constrains the system to three eigenstates with spin parity $3/2^-$ or $1/2^-$, and due to the exclusion of scattering states, our predictions for compact pentaquarks are more limited. Similar to the previous cases, the color-spin bases outlined in Appendix A, along with the relations

$$\begin{aligned} \gamma_{\Omega\Upsilon} &= \gamma_{\Omega\eta_b}, \qquad \gamma_{\Omega J/\psi} = \gamma_{\Omega\eta_c}, \\ \gamma_{\Omega_b^* B_s^*} &= \gamma_{\Omega_b^* B_s} = \gamma_{\Omega_b B_s^*} = \gamma_{\Omega_b B_s}, \\ \gamma_{\Omega_c^* D_s^*} &= \gamma_{\Omega_c^* D_s} = \gamma_{\Omega_c D_s^*} = \gamma_{\Omega_c D_s}, \end{aligned} \tag{20}$$

are employed to evaluate hadron properties of $sssQ\bar{Q}$. The numerical results are detailed in Tables VII and VIII.

In this context, we characterize a $sssQ\bar{Q}$ pentaquark state using the notation $P_{Qsss}(J^P, M)$. Notably, the bottom system features $P_{bsss}(1/2^-, 11.823)$, $P_{bsss}(1/2^-, 11.860)$, and $P_{bsss}(3/2^-, 11.841)$. The lightest and heaviest states of P_{csss} are $P_{csss}(1/2^-, 4.953)$ and $P_{csss}(1/2^-, 5.126)$, respectively. We predict that the P_{Qsss} states with $J^P = 1/2^-$ can be discovered in channel $\Omega\Upsilon$ ($\Omega J/\psi$), and those of $3/2^-$ are anticipated in $\Omega\eta_b$ ($\Omega\eta_c$). Additionally, we explore the ratios of partial widths in the coupling $ssQ \otimes s\bar{Q}$, where the state $P_{csss}(1/2^-, 5.037)$ exhibits a dominant channel in $\Omega_c D_s^*$. These features provide insights for predicting the spin parity of pentaquarks based on reported decay channels.

TABLE VII. Calculated spectra (in GeV) of pentaquarks $sssb\bar{b}$. Bag radius R_0 is in GeV^{-1}. Magnetic moments are in units of μ_N. The numbers below respective decay channels are ratios of partial width. The states denoted by asterisks couple strongly to scattering states.

	$sssb\bar{b}$			$sss \otimes b\bar{b}$		$ssb \otimes s\bar{b}$			
J^P	R_0	M	μ	$\Omega\Upsilon$	$\Omega\eta_b$	$\Omega_b^* B_s^*$	$\Omega_b^* B_s$	$\Omega_b B_s^*$	$\Omega_b B_s$
$5/2^-$	5.63	11.673		*					
$3/2^-$	5.65	11.841	−0.76	0	1	1	0.56	0.18	
	5.63	11.673		*					
	5.62	11.668			*				
$1/2^-$	5.69	11.860	−0.39	1		1		0.14	0.03
	5.62	11.823	−0.11	1		1		16.21	6.56
	5.62	11.671		*					

TABLE VIII. Calculated spectra (in GeV) of pentaquarks $sssc\bar{c}$. Bag radius R_0 is in GeV^{-1}. Magnetic moments are in units of μ_N. The numbers below respective decay channels are ratios of partial width. The states denoted by asterisks couple strongly to scattering states.

	$sssc\bar{c}$			$sss \otimes c\bar{c}$		$ssc \otimes s\bar{c}$			
J^P	R_0	M	μ	$\Omega J/\psi$	$\Omega\eta_c$	$\Omega_c^* D_s^*$	$\Omega_c^* D_s$	$\Omega_c D_s^*$	$\Omega_c D_s$
$5/2^-$	5.90	4.987		*					
$3/2^-$	5.93	5.076	−0.91	0	1	1	0.45	0.09	
	5.90	4.987		*					
	5.80	4.940			*				
$1/2^-$	6.00	5.126	0.05	1		1		0.05	0.01
	5.88	5.037	−0.64	1		1		326.17	33.47
	5.82	4.953	−1.20	1		1		0.87	31.37

IV. SUMMARY

In this work, hidden-heavy pentaquarks P_Q with strangeness $S = 0, -1, -2, -3$ are studied systematicallly using the unified framework of MIT bag model with enhanced heavy-flavor bindings and two-body decay formula of them. With the help of color-spin bases expressed in terms of Young tableau and Young-Yamanouchi bases for the $SU_c(3) \otimes SU_s(2)$ group, we computed the masses and magnetic moments of the hidden-heavy pentaquarks considered. The obtained component amplitudes (eigenvectors) of the two-body $1_c \otimes 1_c$ bases (baryon-meson coupling) in the color-spin wave function of the pentaquarks are employed to predict the relative widths of these pentaquarks decaying into the respective baryon-meson final states. We find that the hidden-heavy pentaquarks have the masses around 4.35–4.90 GeV for the P_{cs}, 11.21–11.67 GeV for the P_{bs}, 4.73–5.02 GeV for the P_{css}, and 11.54–11.77 GeV for the P_{bss}.

For the nonstrange P_Q states with $J^P = 1/2^-$, the computed mass around 4.45–4.82 GeV (Table II) for the P_c states and the 11.31–11.58 GeV (Table I) for the P_b states are all above the observed masses of the LHCb-reported P_c resonances. This implies noncompact features of these reported resonances, as commonly suggested, and that one has to search compact P_c states preferably above 4.45 GeV in the channels of the NJ/ψ and $N\eta_c$ systems. For the singly strange P_{cs} states, the LHCb-reported candidate $P^{\Lambda}_{\psi s}(4338)^0$ is in consistent with the prediction $P_{cs}(4353, 1/2^-)$ (Table IV), while around 4459 MeV, the P_{cs} state is found to contain two substructures, one at 4487 MeV with $J^P = 1/2^-$ and the other at 4494 MeV with $3/2^-$, as indicated by experimental discovery of the state $P_{cs}(4459)^0$. We hope the future measurements involving the decay channels $N\eta_c$ and $\Lambda\eta_c$ to test the computed relative widths of the hidden-charm pentaquarks.

Due to correspondence with charge of the final states, the calculated information of the magnetic moments, arranged by the third component of isospin in this work, is also useful for identification of the respective hadronic states. We hope that the computed hadron properties including decay behaviors can provide guidance in searching for the hidden-heavy pentaquarks in the near future.

ACKNOWLEDGMENTS

W. Z. thanks Hong-Tao An for useful discussions on wave functions and partial width, and Wen-Nian Liu for valuable comments about pentaquark candidates. D. J. is supported by the National Natural Science Foundation of China under Grant No. 12165017.

APPENDIX A: COLOR AND SPIN WAVE FUNCTIONS

For numerical calculations of masses and magnetic moments, it is essential to employ color-spin wave functions to describe the chromomagnetic structure of a given pentaquark state. In the context of hidden-heavy pentaquarks with three light degrees of freedom, indicating flavor symmetry up to three identical quarks, the Young tableau is employed to represent color and spin wave functions in terms of the Young-Yamanouchi bases. The use of Young tableau and the SU(3) permutation group for color representations and its application to various pentaquark systems has been discussed and implemented in the literatures; see Refs. [44,56,65–67], for instance.

The color wave functions in the configuration $q_1q_2q_3q_4\bar{q}_5$ constrained by overall color confinement are selected in color singlets through the application of the Young tableau. These wave functions are expressed as follows:

$$\begin{array}{|c|c|}\hline 1&2\\\hline 3\\\cline{1-1}4\\\cline{1-1}\end{array}\otimes\bar{5}\;\phi_1\;,\quad \begin{array}{|c|c|}\hline 1&3\\\hline 2\\\cline{1-1}4\\\cline{1-1}\end{array}\otimes\bar{5}\;\phi_2\;,\quad \begin{array}{|c|c|}\hline 1&4\\\hline 2\\\cline{1-1}3\\\cline{1-1}\end{array}\otimes\bar{5}\;\phi_3\;. \tag{A1}$$

Note that, in this work, particular attention is given to the third color basis denoted as ϕ_3, which serves to couple the color-singlet wave functions of the baryon and meson, resulting in $(q_1q_2q_3) \otimes (q_4\bar{q}_5)$. This specific coupling corresponds to the unstable scattering state and final states of the OZI-superallowed decay mode.

Similarly, spin wave functions can be expressed in terms of Young tableau [5], [4,1], and [3,2] and classified into spin multiplets. For the pentaquark with spin $J = 5/2$, there is one basis

$$\begin{array}{|c|c|c|c|c|}\hline 1&2&3&4&5\\\hline\end{array}_{\chi_1}. \tag{A2}$$

In the case of the $J = 3/2$, the spin wave functions are

$$\begin{array}{|c|c|c|c|}\hline 1&2&3&4\\\hline 5\\\cline{1-1}\end{array}_{\chi_2}, \begin{array}{|c|c|c|c|}\hline 1&2&3&5\\\hline 4\\\cline{1-1}\end{array}_{\chi_3}, \begin{array}{|c|c|c|c|}\hline 1&2&4&5\\\hline 3\\\cline{1-1}\end{array}_{\chi_4}, \begin{array}{|c|c|c|c|}\hline 1&3&4&5\\\hline 2\\\cline{1-1}\end{array}_{\chi_5}, \tag{A3}$$

and for $J = 1/2$, they become

$$\begin{array}{|c|c|c|}\hline 1&2&3\\\hline 4&5\\\cline{1-2}\end{array}_{\chi_6}, \begin{array}{|c|c|c|}\hline 1&2&4\\\hline 3&5\\\cline{1-2}\end{array}_{\chi_7}, \begin{array}{|c|c|c|}\hline 1&3&4\\\hline 2&5\\\cline{1-2}\end{array}_{\chi_8}, \begin{array}{|c|c|c|}\hline 1&2&5\\\hline 3&4\\\cline{1-2}\end{array}_{\chi_9}, \begin{array}{|c|c|c|}\hline 1&3&5\\\hline 2&4\\\cline{1-2}\end{array}_{\chi_{10}}. \tag{A4}$$

In addition to their role in calculating chromomagnetic interactions, these spin wave functions are sufficient to derive matrix elements of magnetic moments as shown in Appendix B, with the help of the following expanding bases:

$$\begin{aligned}
\chi_1 &= \uparrow\uparrow\uparrow\uparrow\uparrow,\\
\chi_2 &= \frac{2}{\sqrt{5}}\uparrow\uparrow\uparrow\uparrow\downarrow - \frac{\sqrt{5}}{10}(\uparrow\uparrow\uparrow\downarrow\uparrow + \uparrow\uparrow\downarrow\uparrow\uparrow + \uparrow\downarrow\uparrow\uparrow\uparrow + \downarrow\uparrow\uparrow\uparrow\uparrow),\\
\chi_3 &= \frac{\sqrt{3}}{2}\uparrow\uparrow\uparrow\downarrow\uparrow - \frac{1}{2\sqrt{3}}(\uparrow\uparrow\downarrow\uparrow\uparrow + \uparrow\downarrow\uparrow\uparrow\uparrow + \downarrow\uparrow\uparrow\uparrow\uparrow),\\
\chi_4 &= \frac{1}{\sqrt{6}}(2\uparrow\uparrow\downarrow\uparrow\uparrow - \uparrow\downarrow\uparrow\uparrow\uparrow - \downarrow\uparrow\uparrow\uparrow\uparrow),\\
\chi_5 &= \frac{1}{\sqrt{2}}(\uparrow\downarrow\uparrow\uparrow\uparrow - \downarrow\uparrow\uparrow\uparrow\uparrow),\\
\chi_6 &= \frac{1}{3\sqrt{2}}(\uparrow\downarrow\downarrow\uparrow\uparrow + \downarrow\uparrow\downarrow\uparrow\uparrow + \downarrow\downarrow\uparrow\uparrow\uparrow - \uparrow\uparrow\downarrow\downarrow\uparrow - \uparrow\downarrow\uparrow\downarrow\uparrow - \downarrow\uparrow\uparrow\downarrow\uparrow - \uparrow\uparrow\downarrow\uparrow\downarrow - \uparrow\downarrow\uparrow\uparrow\downarrow - \downarrow\uparrow\uparrow\uparrow\downarrow) + \frac{1}{\sqrt{2}}\uparrow\uparrow\uparrow\downarrow\downarrow,\\
\chi_7 &= \frac{1}{3}(2\uparrow\uparrow\downarrow\uparrow\downarrow - \uparrow\downarrow\uparrow\uparrow\downarrow - \downarrow\uparrow\uparrow\uparrow\downarrow - \uparrow\uparrow\downarrow\downarrow\uparrow + \downarrow\downarrow\uparrow\uparrow\uparrow) + \frac{1}{6}(\uparrow\downarrow\uparrow\downarrow\uparrow - \uparrow\downarrow\downarrow\uparrow\uparrow - \downarrow\uparrow\downarrow\uparrow\uparrow + \downarrow\uparrow\uparrow\downarrow\uparrow),\\
\chi_8 &= \frac{1}{\sqrt{3}}(\uparrow\downarrow\uparrow\uparrow\downarrow - \downarrow\uparrow\uparrow\uparrow\downarrow) - \frac{1}{2\sqrt{3}}(\uparrow\downarrow\uparrow\downarrow\uparrow + \uparrow\downarrow\downarrow\uparrow\uparrow - \downarrow\uparrow\downarrow\uparrow\uparrow - \downarrow\uparrow\uparrow\downarrow\uparrow),\\
\chi_9 &= \frac{1}{\sqrt{3}}(\uparrow\uparrow\downarrow\downarrow\uparrow + \downarrow\downarrow\uparrow\uparrow\uparrow) - \frac{1}{2\sqrt{3}}(\uparrow\downarrow\uparrow\downarrow\uparrow + \uparrow\downarrow\downarrow\uparrow\uparrow + \downarrow\uparrow\downarrow\uparrow\uparrow + \downarrow\uparrow\uparrow\downarrow\uparrow),\\
\chi_{10} &= \frac{1}{2}(\uparrow\downarrow\uparrow\downarrow\uparrow - \uparrow\downarrow\downarrow\uparrow\uparrow + \downarrow\uparrow\downarrow\uparrow\uparrow - \downarrow\uparrow\uparrow\downarrow\uparrow).
\end{aligned} \tag{A5}$$

Given the color and spin wave functions (A1), (A2), (A3), and (A4), it becomes possible to construct 30 color-spin bases by performing the product of Young tableaux:

$$\begin{aligned}
&\begin{array}{|c|}\hline 1\\\hline 2\\\hline 3\\\hline 4\\\hline\end{array}\psi'_1,\psi_1, \begin{array}{|c|c|c|}\hline 1&3&4\\\hline 2\\\cline{1-1}\end{array}\psi'_7,\psi_7,\psi_{13}, \begin{array}{|c|c|}\hline 1&4\\\hline 2\\\hline 3\\\cline{1-2}\end{array}\psi^*_3,\psi'_3,\psi'_{11},\psi_3,\psi_{11},\\
&\begin{array}{|c|c|}\hline 1&3\\\hline 2&4\\\cline{1-2}\end{array}\psi'_6,\psi_6, \begin{array}{|c|c|c|}\hline 1&2&4\\\hline 3\\\cline{1-1}\end{array}\psi'_8,\psi_8,\psi_{14}, \begin{array}{|c|c|}\hline 1&3\\\hline 2\\\hline 4\\\cline{1-2}\end{array}\psi^*_2,\psi'_4,\psi'_{12},\psi_4,\psi_{12},\\
&\begin{array}{|c|c|}\hline 1&2\\\hline 3&4\\\cline{1-2}\end{array}\psi'_5,\psi_5, \begin{array}{|c|c|c|}\hline 1&2&3\\\hline 4\\\cline{1-1}\end{array}\psi'_9,\psi_9,\psi_{15}, \begin{array}{|c|c|}\hline 1&2\\\hline 3\\\hline 4\\\cline{1-2}\end{array}\psi^*_1,\psi'_2,\psi'_{10},\psi_2,\psi_{10}.
\end{aligned} \tag{A6}$$

TABLE IX. Color-spin wave functions of hidden-heavy pentaquarks with isospin I and quantum number J^P.

System	I	J^P	Color-spin wave functions
$nnnQ\bar{Q}$, $sssQ\bar{Q}$	3/2	$5/2^-$	ψ_3^*
		$3/2^-$	ψ_1', ψ_3', ψ_{11}'
		$1/2^-$	ψ_1, ψ_3, ψ_{11}
$nnnQ\bar{Q}$	1/2	$5/2^-$	$\frac{1}{\sqrt{2}}\psi_2^* - \frac{1}{\sqrt{2}}\psi_1^*$
		$3/2^-$	$\frac{1}{\sqrt{2}}\psi_4' - \frac{1}{\sqrt{2}}\psi_2'$, $\frac{1}{\sqrt{2}}\psi_6' - \frac{1}{\sqrt{2}}\psi_5'$, $\frac{1}{\sqrt{2}}\psi_7' - \frac{1}{\sqrt{2}}\psi_8'$, $\frac{1}{\sqrt{2}}\psi_{12}' - \frac{1}{\sqrt{2}}\psi_{10}'$
		$1/2^-$	$\frac{1}{\sqrt{2}}\psi_4 - \frac{1}{\sqrt{2}}\psi_2$, $\frac{1}{\sqrt{2}}\psi_6 - \frac{1}{\sqrt{2}}\psi_5$, $\frac{1}{\sqrt{2}}\psi_7 - \frac{1}{\sqrt{2}}\psi_8$, $\frac{1}{\sqrt{2}}\psi_{12} - \frac{1}{\sqrt{2}}\psi_{10}$, $\frac{1}{\sqrt{2}}\psi_{13} - \frac{1}{\sqrt{2}}\psi_{14}$
$nnsQ\bar{Q}$, $ssnQ\bar{Q}$	1	$5/2^-$	ψ_2^*, ψ_3^*
		$3/2^-$	ψ_1', ψ_3', ψ_4', ψ_6', ψ_7', ψ_{11}', ψ_{12}'
		$1/2^-$	ψ_1, ψ_3, ψ_4, ψ_6, ψ_7, ψ_{11}, ψ_{12}, ψ_{13}
$nnsQ\bar{Q}$	0	$5/2^-$	ψ_1^*
		$3/2^-$	ψ_2', ψ_5', ψ_8', ψ_9', ψ_{10}'
		$1/2^-$	ψ_2, ψ_5, ψ_8, ψ_9, ψ_{10}, ψ_{14}, ψ_{15}

Due to the Pauli's principle, the wave function is inherently fully antisymmetric under the exchange of any pair among the four quarks q_1, q_2, q_3, and q_4. This foundational property allows for the selection of physically possible bases from Eq. (A6) for any pentaquark state with a specific flavor configuration and quantum numbers IJ^P. These bases are organized and detailed in Table IX. The explicit expressions of them, as given in Eqs. (A7)–(A34), are employed for the computation of masses and magnetic moments. It is noteworthy that these bases are equivalent to that outlined in Ref. [35] in numerical calculations, which allows the evaluation of eigenvectors for partial width studies.

(1) $J^P = 5/2^-$

$$\psi_1^* = \phi_1\chi_1, \qquad \psi_2^* = \phi_2\chi_1, \qquad \psi_3^* = \phi_3\chi_1. \tag{A7}$$

(2) $J^P = 3/2^-$

$$\psi_1' = \frac{1}{\sqrt{3}}\phi_1\chi_5 - \frac{1}{\sqrt{3}}\phi_2\chi_4 + \frac{1}{\sqrt{3}}\phi_3\chi_3, \tag{A8}$$

$$\psi_2' = -\frac{1}{\sqrt{6}}\phi_1\chi_3 - \frac{1}{\sqrt{3}}\phi_1\chi_4 + \frac{1}{\sqrt{3}}\phi_2\chi_5 - \frac{1}{\sqrt{6}}\phi_3\chi_5, \tag{A9}$$

$$\psi_3' = -\frac{1}{\sqrt{6}}\phi_1\chi_5 + \frac{1}{\sqrt{6}}\phi_2\chi_4 + \sqrt{\frac{2}{3}}\phi_3\chi_3, \tag{A10}$$

$$\psi_4' = \frac{1}{\sqrt{3}}\phi_1\chi_5 - \frac{1}{\sqrt{6}}\phi_2\chi_3 + \frac{1}{\sqrt{3}}\phi_2\chi_4 + \frac{1}{\sqrt{6}}\phi_3\chi_4, \tag{A11}$$

$$\psi_5' = -\frac{1}{\sqrt{3}}\phi_1\chi_3 + \frac{1}{\sqrt{6}}\phi_1\chi_4 - \frac{1}{\sqrt{6}}\phi_2\chi_5 - \frac{1}{\sqrt{3}}\phi_3\chi_5, \tag{A12}$$

$$\psi_6' = -\frac{1}{\sqrt{6}}\phi_1\chi_5 - \frac{1}{\sqrt{3}}\phi_2\chi_3 - \frac{1}{\sqrt{6}}\phi_2\chi_4 + \frac{1}{\sqrt{3}}\phi_3\chi_4, \tag{A13}$$

$$\psi_7' = -\frac{1}{\sqrt{2}}\phi_2\chi_3 - \frac{1}{\sqrt{2}}\phi_3\chi_4, \tag{A14}$$

$$\psi_8' = -\frac{1}{\sqrt{2}}\phi_1\chi_3 + \frac{1}{\sqrt{2}}\phi_3\chi_5, \tag{A15}$$

$$\psi_9' = \frac{1}{\sqrt{2}}\phi_1\chi_4 + \frac{1}{\sqrt{2}}\phi_2\chi_5, \tag{A16}$$

$$\psi_{10}' = \phi_1\chi_2, \tag{A17}$$

$$\psi_{11}' = \phi_3\chi_2, \tag{A18}$$

$$\psi_{12}' = \phi_2\chi_2. \tag{A19}$$

(3) $J^P = 1/2^-$

$$\psi_1 = \frac{1}{\sqrt{3}}\phi_1\chi_8 - \frac{1}{\sqrt{3}}\phi_2\chi_7 + \frac{1}{\sqrt{3}}\phi_3\chi_6, \tag{A20}$$

$$\psi_2 = -\frac{1}{\sqrt{6}}\phi_1\chi_6 - \frac{1}{\sqrt{3}}\phi_1\chi_7 + \frac{1}{\sqrt{3}}\phi_2\chi_8 - \frac{1}{\sqrt{6}}\phi_3\chi_8, \tag{A21}$$

$$\psi_3 = -\frac{1}{\sqrt{6}}\phi_1\chi_8 + \frac{1}{\sqrt{6}}\phi_2\chi_7 + \sqrt{\frac{2}{3}}\phi_3\chi_6, \tag{A22}$$

$$\psi_4 = \frac{1}{\sqrt{3}}\phi_1\chi_8 - \frac{1}{\sqrt{6}}\phi_2\chi_6 + \frac{1}{\sqrt{3}}\phi_2\chi_7 + \frac{1}{\sqrt{6}}\phi_3\chi_7, \tag{A23}$$

$$\psi_5 = -\frac{1}{\sqrt{3}}\phi_1\chi_6 + \frac{1}{\sqrt{6}}\phi_1\chi_7 - \frac{1}{\sqrt{6}}\phi_2\chi_8 - \frac{1}{\sqrt{3}}\phi_3\chi_8, \tag{A24}$$

$$\psi_6 = -\frac{1}{\sqrt{6}}\phi_1\chi_8 - \frac{1}{\sqrt{3}}\phi_2\chi_6 - \frac{1}{\sqrt{6}}\phi_2\chi_7 + \frac{1}{\sqrt{3}}\phi_3\chi_7, \tag{A25}$$

$$\psi_7 = -\frac{1}{\sqrt{2}}\phi_2\chi_6 - \frac{1}{\sqrt{2}}\phi_3\chi_7, \tag{A26}$$

$$\psi_8 = -\frac{1}{\sqrt{2}}\phi_1\chi_6 + \frac{1}{\sqrt{2}}\phi_3\chi_8, \tag{A27}$$

$$\psi_9 = \frac{1}{\sqrt{2}}\phi_1\chi_7 + \frac{1}{\sqrt{2}}\phi_2\chi_8, \tag{A28}$$

$$\psi_{10} = -\frac{1}{2}\phi_1\chi_9 + \frac{1}{2}\phi_2\chi_{10} + \frac{1}{\sqrt{2}}\phi_3\chi_{10}, \tag{A29}$$

$$\psi_{11} = \frac{1}{\sqrt{2}}\phi_1\chi_{10} - \frac{1}{\sqrt{2}}\phi_2\chi_9, \tag{A30}$$

$$\psi_{12} = \frac{1}{2}\phi_1\chi_{10} + \frac{1}{2}\phi_2\chi_9 - \frac{1}{\sqrt{2}}\phi_3\chi_9, \tag{A31}$$

$$\psi_{13} = -\frac{1}{2}\phi_1\chi_{10} - \frac{1}{2}\phi_2\chi_9 - \frac{1}{\sqrt{2}}\phi_3\chi_9, \tag{A32}$$

$$\psi_{14} = \frac{1}{2}\phi_1\chi_9 - \frac{1}{2}\phi_2\chi_{10} + \frac{1}{\sqrt{2}}\phi_3\chi_{10}, \tag{A33}$$

$$\psi_{15} = -\frac{1}{\sqrt{2}}\phi_1\chi_9 - \frac{1}{\sqrt{2}}\phi_2\chi_{10}. \tag{A34}$$

APPENDIX B: MAGNETIC MOMENTS

In this section, we will exhibit the process by which the magnetic moments of pentaquarks are derived. The inspiration for our method is drawn from Eq. (7), motivating a computation approach grounded in basic quantum mechanics, where the physical quantity is considered as the average value of an operator. For hadronic states, the operator $\hat{\mu}$ is applicable solely to the spin components of the wave function, resulting in the neglect of orbital and flavor parts, which are treated as orthogonal. Consequently, in the presence of chromomagnetic mixing, it becomes reasonable to utilize the color-spin bases from Table IX for the computation of the average value of the operator $\hat{\mu}$.

After finishing the study of masses for given pentaquark states with color-spin bases, the results yield two types of quantities: the magnetic moments for individual quarks μ_i and eigenvectors $(C_1, C_2, \ldots)$. Considering the example of the system $sssQ\bar{Q}$ with $J = 3/2$, the associated color-spin wave function is expressed as $\psi = C_1\psi'_1 + C_2\psi'_3 + C_3\psi'_{11}$, where the eigenvector is calculated to be (C_1, C_2, C_3). This information allows us to derive the expression for the magnetic moment through the following steps:

$$\begin{aligned}
\mu &= \langle\psi|\hat{\mu}|\psi\rangle \\
&= C_1^2\langle\psi'_1|\hat{\mu}|\psi'_1\rangle + C_2^2\langle\psi'_3|\hat{\mu}|\psi'_3\rangle + C_3^2\langle\psi'_{11}|\hat{\mu}|\psi'_{11}\rangle + 2C_1C_2\langle\psi'_1|\hat{\mu}|\psi'_3\rangle + 2C_1C_3\langle\psi'_1|\hat{\mu}|\psi'_{11}\rangle + 2C_2C_3\langle\psi'_3|\hat{\mu}|\psi'_{11}\rangle \\
&= C_1^2\left\langle\frac{1}{\sqrt{3}}\phi_1\chi_5 - \frac{1}{\sqrt{3}}\phi_2\chi_4 + \frac{1}{\sqrt{3}}\phi_3\chi_3|\hat{\mu}|\frac{1}{\sqrt{3}}\phi_1\chi_5 - \frac{1}{\sqrt{3}}\phi_2\chi_4 + \frac{1}{\sqrt{3}}\phi_3\chi_3\right\rangle \\
&\quad + C_2^2\left\langle-\frac{1}{\sqrt{6}}\phi_1\chi_5 + \frac{1}{\sqrt{6}}\phi_2\chi_4 + \sqrt{\frac{2}{3}}\phi_3\chi_3|\hat{\mu}|-\frac{1}{\sqrt{6}}\phi_1\chi_5 + \frac{1}{\sqrt{6}}\phi_2\chi_4 + \sqrt{\frac{2}{3}}\phi_3\chi_3\right\rangle + C_3^2\langle\phi_3\chi_2|\hat{\mu}|\phi_3\chi_2\rangle \\
&\quad + 2C_1C_2\left\langle\frac{1}{\sqrt{3}}\phi_1\chi_5 - \frac{1}{\sqrt{3}}\phi_2\chi_4 + \frac{1}{\sqrt{3}}\phi_3\chi_3|\hat{\mu}|-\frac{1}{\sqrt{6}}\phi_1\chi_5 + \frac{1}{\sqrt{6}}\phi_2\chi_4 + \sqrt{\frac{2}{3}}\phi_3\chi_3\right\rangle \\
&\quad + 2C_1C_3\left\langle\frac{1}{\sqrt{3}}\phi_1\chi_5 - \frac{1}{\sqrt{3}}\phi_2\chi_4 + \frac{1}{\sqrt{3}}\phi_3\chi_3|\hat{\mu}|\phi_3\chi_2\right\rangle + 2C_2C_3\left\langle-\frac{1}{\sqrt{6}}\phi_1\chi_5 + \frac{1}{\sqrt{6}}\phi_2\chi_4 + \sqrt{\frac{2}{3}}\phi_3\chi_3|\hat{\mu}|\phi_3\chi_2\right\rangle \\
&= \left(\frac{1}{3}C_1^2 + \frac{1}{6}C_2^2 - \frac{\sqrt{2}}{3}C_1C_2\right)\langle\chi_5|\hat{\mu}|\chi_5\rangle + \left(\frac{1}{3}C_1^2 + \frac{1}{6}C_2^2 - \frac{\sqrt{2}}{3}C_1C_2\right)\langle\chi_4|\hat{\mu}|\chi_4\rangle + \left(\frac{1}{3}C_1^2 + \frac{2}{3}C_2^2 + \frac{2\sqrt{2}}{3}C_1C_2\right)\langle\chi_3|\hat{\mu}|\chi_3\rangle \\
&\quad + \left(\frac{2}{\sqrt{3}}C_1C_3 + 2\sqrt{\frac{2}{3}}C_2C_3\right)\langle\chi_3|\hat{\mu}|\chi_2\rangle + C_3^2\langle\chi_2|\hat{\mu}|\chi_2\rangle.
\end{aligned} \tag{B1}$$

TABLE X. Matrix elements of magnetic moments $\langle\chi_i|\hat{\mu}|\chi_j\rangle$ in spin subspace $(\chi_1, \chi_2, \chi_3, \chi_4, \chi_5)$.

Spin	χ_1	χ_2	χ_3	χ_4	χ_5
χ_1	$\mu_1+\mu_2+\mu_3+\mu_4+\mu_5$	0	0	0	0
χ_2	0	$\frac{9}{10}(\mu_1+\mu_2+\mu_3+\mu_4)-\frac{3}{5}\mu_5$	$-\frac{\sqrt{15}}{30}(\mu_1+\mu_2+\mu_3-3\mu_4)$	$-\frac{\sqrt{30}}{30}(\mu_1+\mu_2-2\mu_3)$	$-\frac{\sqrt{10}}{10}(\mu_1-\mu_2)$
χ_3	0	$-\frac{\sqrt{15}}{30}(\mu_1+\mu_2+\mu_3-3\mu_4)$	$\frac{5}{6}(\mu_1+\mu_2+\mu_3)-\frac{1}{2}\mu_4+\mu_5$	$-\frac{\sqrt{2}}{6}(\mu_1+\mu_2-2\mu_3)$	$-\frac{\sqrt{6}}{6}(\mu_1-\mu_2)$
χ_4	0	$-\frac{\sqrt{30}}{30}(\mu_1+\mu_2-2\mu_3)$	$-\frac{\sqrt{2}}{6}(\mu_1+\mu_2-2\mu_3)$	$\frac{1}{3}(2\mu_1+2\mu_2-\mu_3)+\mu_4+\mu_5$	$-\frac{\sqrt{3}}{3}(\mu_1-\mu_2)$
χ_5	0	$-\frac{\sqrt{10}}{10}(\mu_1-\mu_2)$	$-\frac{\sqrt{6}}{6}(\mu_1-\mu_2)$	$-\frac{\sqrt{3}}{3}(\mu_1-\mu_2)$	$\mu_3+\mu_4+\mu_5$

TABLE XI. Matrix elements of magnetic moments $\langle\chi_i|\hat{\mu}|\chi_j\rangle$ in spin subspace $(\chi_6, \chi_7, \chi_8, \chi_9, \chi_{10})$.

Spin	χ_6	χ_7	χ_8	χ_9	χ_{10}
χ_6	$\frac{1}{9}(5\mu_1+5\mu_2+5\mu_3-3\mu_4-3\mu_5)$	$-\frac{\sqrt{2}}{9}(\mu_1+\mu_2-2\mu_3)$	$-\frac{\sqrt{6}}{9}(\mu_1-\mu_2)$	$-\frac{\sqrt{6}}{9}(\mu_1+\mu_2-2\mu_3)$	$-\frac{\sqrt{2}}{3}(\mu_1-\mu_2)$
χ_7	$-\frac{\sqrt{2}}{9}(\mu_1+\mu_2-2\mu_3)$	$\frac{1}{9}(4\mu_1+4\mu_2-2\mu_3+6\mu_4-3\mu_5)$	$-\frac{2\sqrt{3}}{9}(\mu_1-\mu_2)$	$-\frac{\sqrt{3}}{9}(2\mu_1+2\mu_2-\mu_3-3\mu_4)$	$\frac{1}{3}(\mu_1-\mu_2)$
χ_8	$-\frac{\sqrt{6}}{9}(\mu_1-\mu_2)$	$-\frac{2\sqrt{3}}{9}(\mu_1-\mu_2)$	$\frac{1}{3}(2\mu_3+2\mu_4-\mu_5)$	$\frac{1}{3}(\mu_1-\mu_2)$	$-\frac{\sqrt{3}}{3}(\mu_3-\mu_4)$
χ_9	$-\frac{\sqrt{6}}{9}(\mu_1+\mu_2-2\mu_3)$	$-\frac{\sqrt{3}}{9}(2\mu_1+2\mu_2-\mu_3-3\mu_4)$	$\frac{1}{3}(\mu_1-\mu_2)$	μ_5	0
χ_{10}	$-\frac{\sqrt{2}}{3}(\mu_1-\mu_2)$	$\frac{1}{3}(\mu_1-\mu_2)$	$-\frac{\sqrt{3}}{3}(\mu_3-\mu_4)$	0	μ_5

In the last step of Eq. (B1), the color bases are orthogonal and neglected, leaving matrix elements $\langle\chi_i|\hat{\mu}|\chi_j\rangle$ in spin space to be determined.

In Tables X and XI, the matrix elements of the magnetic moment in spin subspaces $(\chi_1, \chi_2, \chi_3, \chi_4, \chi_5)$ and $(\chi_6, \chi_7, \chi_8, \chi_9, \chi_{10})$, respectively, are provided directly. These matrix elements are determined with the assistance of the spin bases given in Eq. (A5). The expressions involve the values μ_i, where the indices i represent flavors in the configuration $q_1q_2q_3q_4\bar{q}_5$, and the μ_i have been calculated previously for individual quarks.

It is important to note that the element is reasonable only if χ_i and χ_j belong to the same spin multiplets, as this is the realm where chromomagnetic mixing occurs. Going forward, these methods can be consistently applied to evaluate magnetic moments for pentaquarks. The availability of color-spin bases, alongside the calculated eigenvectors and μ_i, facilitates this systematic approach.

[1] M. Gell-Mann, Phys. Lett. **8**, 214 (1964).
[2] G. Zweig, Report No. CERN-TH-401, 1964.
[3] R. L. Jaffe, Phys. Rev. D **15**, 267 (1977).
[4] R. L. Jaffe, Phys. Rev. D **15**, 281 (1977).
[5] T. A. DeGrand, R. L. Jaffe, K. Johnson, and J. E. Kiskis, Phys. Rev. D **12**, 2060 (1975).
[6] S. Fleck and J. M. Richard, Prog. Theor. Phys. **82**, 760 (1989).
[7] D.-H. He, K. Qian, Y.-B. Ding, X.-Q. Li, and P.-N. Shen, Phys. Rev. D **70**, 094004 (2004).
[8] A. Bernotas and V. Simonis, Lith. J. Phys. **49**, 19 (2009).
[9] A. Bernotas and V. Simonis, Lith. J. Phys. **53**, 84 (2012).
[10] D. Strottman, Phys. Rev. D **20**, 748 (1979).
[11] T. Barnes, F. E. Close, and F. de Viron, Nucl. Phys. **B224**, 241 (1983).
[12] M. S. Chanowitz and S. R. Sharpe, Nucl. Phys. **B222**, 211 (1983); **228**, 588(E) (1983).
[13] S. K. Choi *et al.* (Belle Collaboration), Phys. Rev. Lett. **91**, 262001 (2003).
[14] M. Ablikim *et al.* (BESIII Collaboration), Phys. Rev. Lett. **110**, 252001 (2013).
[15] Z. Q. Liu *et al.* (Belle Collaboration), Phys. Rev. Lett. **110**, 252002 (2013); **111**, 019901(E) (2013).
[16] R. Aaij *et al.* (LHCb Collaboration), Nat. Commun. **13**, 3351 (2022).
[17] A. Hayrapetyan *et al.* (CMS Collaboration), Phys. Rev. Lett. **132** (2024) 111901.
[18] R. Aaij *et al.* (LHCb Collaboration), Sci. Bull. **65**, 1983 (2020).
[19] R. Aaij *et al.* (LHCb Collaboration), Phys. Rev. Lett. **115**, 072001 (2015).
[20] R. Aaij *et al.* (LHCb Collaboration), Phys. Rev. Lett. **131**, 031901 (2023).
[21] R. Aaij *et al.* (LHCb Collaboration), Sci. Bull. **66**, 1278 (2021).
[22] H.-X. Chen, W. Chen, X. Liu, and X.-H. Liu, Eur. Phys. J. C **81**, 409 (2021).
[23] R. Chen, Phys. Rev. D **103**, 054007 (2021).

[24] F. Yang, Y. Huang, and H. Q. Zhu, Sci. China Phys. Mech. Astron. **64**, 121011 (2021).
[25] J.-X. Lu, M.-Z. Liu, R.-X. Shi, and L.-S. Geng, Phys. Rev. D **104**, 034022 (2021).
[26] C. W. Xiao, J. J. Wu, and B. S. Zou, Phys. Rev. D **103**, 054016 (2021).
[27] J.-T. Zhu, L.-Q. Song, and J. He, Phys. Rev. D **103**, 074007 (2021).
[28] A. Feijoo, W.-F. Wang, C.-W. Xiao, J.-J. Wu, E. Oset, J. Nieves, and B.-S. Zou, Phys. Lett. B **839**, 137760 (2023).
[29] J.-T. Zhu, S.-Y. Kong, and J. He, Phys. Rev. D **107**, 034029 (2023).
[30] K. Chen, Z.-Y. Lin, and S.-L. Zhu, Phys. Rev. D **106**, 116017 (2022).
[31] F.-L. Wang and X. Liu, Phys. Lett. B **835**, 137583 (2022).
[32] F.-L. Wang and X. Liu, Phys. Rev. D **108**, 054028 (2023).
[33] K. Azizi, Y. Sarac, and H. Sundu, Phys. Rev. D **108**, 074010 (2023).
[34] M.-W. Li, Z.-W. Liu, Z.-F. Sun, and R. Chen, Phys. Rev. D **104**, 054016 (2021).
[35] X.-Z. Weng, X.-L. Chen, W.-Z. Deng, and S.-L. Zhu, Phys. Rev. D **100**, 016014 (2019).
[36] P.-P. Shi, F. Huang, and W.-L. Wang, Eur. Phys. J. A **57**, 237 (2021).
[37] W. Ruangyoo, K. Phumphan, C.-C. Chen, A. Limphirat, and Y. Yan, J. Phys. G **49**, 075001 (2022).
[38] S.-Y. Li, Y.-R. Liu, Z.-L. Man, Z.-G. Si, and J. Wu, Phys. Rev. D **108**, 056015 (2023).
[39] F. Guo and H.-S. Li, Eur. Phys. J. C **84**, 392 (2024).
[40] G. Yang, J. Ping, and J. Segovia, Phys. Rev. D **99**, 014035 (2019).
[41] J.-T. Zhu, S.-Y. Kong, Y. Liu, and J. He, Eur. Phys. J. C **80**, 1016 (2020).
[42] W.-X. Zhang, H. Xu, and D. Jia, Phys. Rev. D **104**, 114011 (2021).
[43] T.-Q. Yan, W.-X. Zhang, and D. Jia, Eur. Phys. J. C **83**, 810 (2023).
[44] W.-X. Zhang, H.-T. An, and D. Jia, Eur. Phys. J. C **83**, 727 (2023).
[45] K. Johnson, Acta Phys. Polon. B **6**, 865 (1975).
[46] M. Karliner and J. L. Rosner, Phys. Rev. D **90**, 094007 (2014).
[47] M. Karliner and J. L. Rosner, Nature (London) **551**, 89 (2017).
[48] M. Karliner and J. L. Rosner, Phys. Rev. Lett. **119**, 202001 (2017).
[49] M. Karliner and J. L. Rosner, Phys. Rev. D **102**, 094016 (2020).
[50] A. De Rujula, H. Georgi, and S. L. Glashow, Phys. Rev. D **12**, 147 (1975).
[51] G.-J. Wang, R. Chen, L. Ma, X. Liu, and S.-L. Zhu, Phys. Rev. D **94**, 094018 (2016).
[52] R. L. Workman *et al.* (Particle Data Group), Prog. Theor. Exp. Phys. **2022**, 083C01 (2022).
[53] E. Tiesinga, P. J. Mohr, D. B. Newell, and B. N. Taylor, Rev. Mod. Phys. **93**, 025010 (2021).
[54] X.-Z. Weng, X.-L. Chen, W.-Z. Deng, and S.-L. Zhu, Phys. Rev. D **103**, 034001 (2021).
[55] X.-Z. Weng, W.-Z. Deng, and S.-L. Zhu, Phys. Rev. D **105**, 034026 (2022).
[56] H.-T. An, K. Chen, and X. Liu, Phys. Rev. D **105**, 034018 (2022).
[57] G. Chong-Shou, *Group Theory and its Application in Particle Physics* (Higher Education Press, Beijing, 1992).
[58] R. Aaij *et al.* (LHCb Collaboration), Phys. Rev. Lett. **122**, 222001 (2019).
[59] R. Aaij *et al.* (LHCb Collaboration), Phys. Rev. Lett. **128**, 062001 (2022).
[60] T. J. Burns and E. S. Swanson, Eur. Phys. J. A **58**, 68 (2022).
[61] X.-Z. Ling, J.-X. Lu, M.-Z. Liu, and L.-S. Geng, Phys. Rev. D **104**, 074022 (2021).
[62] M.-L. Du, V. Baru, F.-K. Guo, C. Hanhart, U.-G. Meißner, J. A. Oller, and Q. Wang, J. High Energy Phys. 08 (2021) 157.
[63] J.-Z. Wang, X. Liu, and T. Matsuki, Phys. Rev. D **104**, 114020 (2021).
[64] R. Chen and X. Liu, Phys. Rev. D **105**, 014029 (2022).
[65] H.-T. An, K. Chen, Z.-W. Liu, and X. Liu, Phys. Rev. D **103**, 074006 (2021).
[66] H.-T. An, K. Chen, Z.-W. Liu, and X. Liu, Phys. Rev. D **103**, 114027 (2021).
[67] H.-T. An, S.-Q. Luo, Z.-W. Liu, and X. Liu, Phys. Rev. D **105**, 074032 (2022).